Assessment of a robust MEMS-based RTK/INS system for UAV applications

Richard Deurloo, Marnix Volckaert, Bei Huang, Kristof Smolders, Valentin Barreau, *Septentrio*

BIOGRAPHIES

Richard Deurloo holds a M.Sc. in Aerospace Engineering from Delft University of Technology in the Netherlands and a Ph.D. in Surveying Engineering from the University of Porto in Portugal. In 2012 he joined Septentrio's R&D department, where he is lead GNSS/INS engineer.

Marnix Volckaert has been with Septentrio's R&D department for 5 years and works on innovative GNSS and INS algorithms. He obtained a M.Sc. in Aerospace Engineering from Delft University of Technology in the Netherlands and a Ph.D. in Mechanical Engineering from the University of Leuven in Belgium.

Bei Huang received the M.Sc. degree in Geomatics Engineering from the University of Calgary, Canada in 2013. She was involved in the research of low-cost multi-sensor integrated navigation. After 4 years as test engineer in a world-leading OEM manufacturer, she joined Septentrio in 2017 and focused on the testing and development for GNSS/INS products.

Kristof Smolders works in the Septentrio R&D department as test engineer since 2012 and is responsible for performance testing of the Septentrio OEM receivers. He obtained a M.Sc. in Mathematics and a Ph.D. in Astronomy from the University of Leuven in Belgium.

Valentin Barreau received his Electronics Engineering degree from ENAC (Ecole Nationale de l'Aviation Civile) in France. He joined Septentrio in 2103 to work as GNSS/INS navigation engineer, responsible for the INS filter performance. In 2018, he started a new challenge at Telespazio France.

ABSTRACT

Recent years has seen a significant increase in UAVs being used in large-scale surveying projects. One reason for this success is that MEMS-based GNSS/INS systems have become available, fitting the strict weight and power budgets of UAV missions as well as driving down the costs. These GNSS/INS systems need to be robust and need to provide reliable and accurate results, in real-time or post-processing, to limit manual corrections and avoid having to re-do surveys.

In this paper we present Septentrio's new RTK/INS solution, specifically developed for UAV survey and inspection applications. In collaboration with a survey UAV manufacturer the performance of the RTK/INS system is assessed onboard a UAV in an environment typical for surveying applications. The performance of the RTK/INS system is compared with other commercially available MEMS-based GNSS/INS systems.

The systems are mounted together on a large X8 octocopter UAV (28 kg). All systems use dual-antenna GNSS receivers and share the same two antennas, separated by a two-meter baseline, for GNSS attitude. The GNSS attitude adds information to the MEMS-based INS filter, which for a multi-copter can improve attitude accuracy during low dynamics (e.g. hovering, straight and level flight) and improves reliability at startup.

A high-grade LiDAR mounted under the UAV provides an application-oriented indirect reference. The LiDAR data collected onboard the UAV is geo-referenced with the position and attitude solutions of each of the GNSS/INS systems under test to generate LiDAR point clouds. In addition, data is collected with the same LiDAR mounted on the ground. This provides a millimeter-accurate geo-referenced model of known structures. The performance of each GNSS/INS solution can be assessed by comparing the accuracy of the UAV-based point clouds with respect to the ground-based point cloud on those features. Since the same LiDAR data is used for each of the GNSS/INS systems, this serves as an independent reference to determine the final geo-referencing accuracy of each of the systems.

INTRODUCTION

In recent years commercial UAVs have moved from niche markets to a fast-growing professional market. UAVs are becoming the standard in large-scale surveying campaigns, serving as platforms for photogrammetry and LiDAR scanning.

For these applications a GNSS/INS system is a must, providing not only timing and position information, but also attitude. In the first place, the position and timing are needed for correct geo-referencing of the collected data. For photogrammetry, attitude can aid in stitching the photographs. For LiDAR scanning applications, high data-rate attitude information is needed to correct for platform motion and to remove artifacts from the point cloud.

The substantial amounts of data produced in these applications do not allow for manual corrections of the sensor data after the measurement campaign or after post-processing. This means that the GNSS/INS system needs to be robust and needs to provide reliable and accurate results, in real-time or post-processing. Robustness in the sense that the system needs to work every time and in all conditions, to limit downtime and to prevent having to re-do part of the measurement campaign. Reliable in the sense that the solution provided by the system needs to be trusted, to limit the need of manual inspection of the data. And accurate to limit degrading the final accuracy of the survey data.

In recent years, GNSS/INS systems based on MEMS IMUs have become available, fitting the strict weight and power budgets of UAV missions as well as driving down the costs. But how accurate and reliable are they really? In this paper we present Septentrio's new GNSS/INS solution, the AsteRx-i, specifically developed for UAV survey and inspection applications. The system was benchmarked against multiple existing commercial MEMS-based GNSS/INS systems.

All systems presented in this paper use dual-antenna GNSS receivers. This adds GNSS attitude information to the INS filter, which can improve attitude accuracy and improves reliability at startup. But the accuracy of the GNSS attitude is highly dependent on the antenna baseline length and on the type of antenna (i.e. high-precision vs. patch antenna). The impact of baseline length and antenna type are therefore briefly discussed. For the UAV benchmark all systems shared the same two antennas.

In collaboration with a survey UAV manufacturer the GNSS/INS systems were benchmarked in a typical environment for survey applications. The systems were mounted on a large quad-copter UAV with a two-meter wide boom for the dual-antenna GNSS receivers. The UAV was equipped with two reference systems: a high-end GNSS/INS system and a high-grade FARO LiDAR. However, the high-end GNSS/INS system failed to provide an accurate solution during our tests due to a software bug. It therefore could not serve as a direct epoch by epoch reference for the systems under test.

The LiDAR data collected with the UAV were post-processed with the position and attitude solutions of each of the GNSS/INS systems under test to generate the LiDAR point cloud. This allows us to compare the accuracy of the point cloud solution for known features and repeated flight lines. In addition, data were collected with the same LiDAR mounted on the ground. This provides a millimeter-accurate geo-referenced model of known structures for absolute reference. Since the same LiDAR data set is used for each of the GNSS/INS systems, this serves as independent reference to determine the accuracy of each of the systems.

In the following sections we first discuss the impact of antenna baseline and antenna type on the GNSS position and attitude, followed by an introduction of the AsteRx-I, Septentrio's new GNSS/INS system. We then provide a description of the test set-up of the UAV flights and a description of the reference data. In the last two sections we present the results and conclusions of the UAV flights.

GNSS POSITIONS AND ATTITUDE

The type of antenna (i.e. high-precision vs. patch antenna) and the antenna baseline length have significant impact on the accuracy of the position and attitude computed by a GNSS receiver. The antenna type determines the (phase) noise level on the GNSS range measurements and, as a result, the accuracy of the GNSS position solution. Patch antennas typically introduce higher noise than high-precision survey-grade antennas. The antenna baseline length determines how much the relative position errors between antennas affect the attitude. For equal relative position errors, a longer baseline will introduce a smaller attitude error than a shorter baseline.

In terrestrial applications, it is often possible to use high-precision antennas and to place these antennas far apart (e.g. 2 m apart). But for a UAV high-precision antennas are too heavy and bulky. And, depending on the size of the UAV, the antenna baseline length may be short (e.g. 50 cm). Therefore, the GNSS position and attitude accuracy are expected to be significantly reduced. It is important to understand this reduction when integrating these GNSS solutions in a GNSS/INS system.

GNSS antenna type comparison

To assess the impact of the antenna type on the GNSS position and attitude, we compared the performance of two antenna types: a patch antenna (Tallysman TW3972) and high-precision antenna (Septentrio PolaNt-MF). We recorded 7 hours of static data with one Septentrio AsteRx-m2a dual antenna GNSS receiver connected to each set of antennas. The data set was recorded in open-sky conditions with an antenna baseline of 2 m. The results show the degradation of performance of the patch antenna compared to the survey-grade antenna.

The position errors for the main antenna in RTK mode are shown in Figure 1 for the two types of antennas. For the patch antenna we include the solutions with and without ground plane (10 cm plane diameter). The RMS values are presented in Table 1.

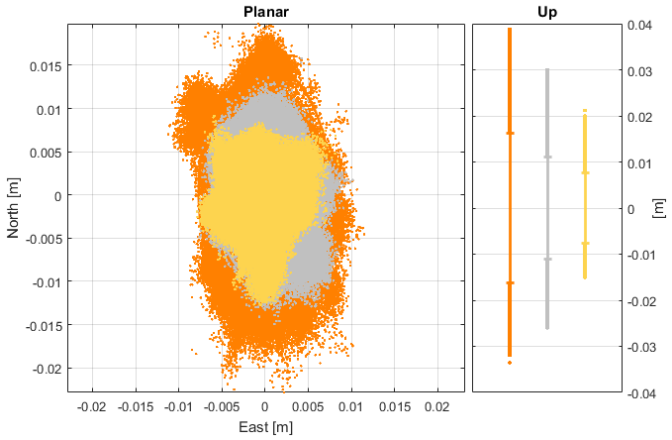

Figure 1: GNSS position errors for PolaNt (green), Tallysman (black), and Tallysman with ground plane (red).

Table 1: GNSS position errors for PolaNt-MF, Tallysman and Tallysman with ground plane.

Antenna type	**Planar RMS (cm)**	**Up RMS (cm)**
PolaNt	0.61	0.47
Tallysman	1.21	0.99
Tallysman + ground plane	0.85	0.68

The RMS of the patch antenna without ground plane is about two times higher than the RMS of the survey antenna. As expected, with the ground plane the RMS of the patch antenna reduces. This shows the importance of using a ground plane with the patch antenna. But the RMS is still 40%-45% higher than the RMS of the survey antenna.

The time plots of the GNSS heading and pitch errors for the patch and survey antennas are shown in Figure 2. The heading and pitch RMS values are shown in Table 2.

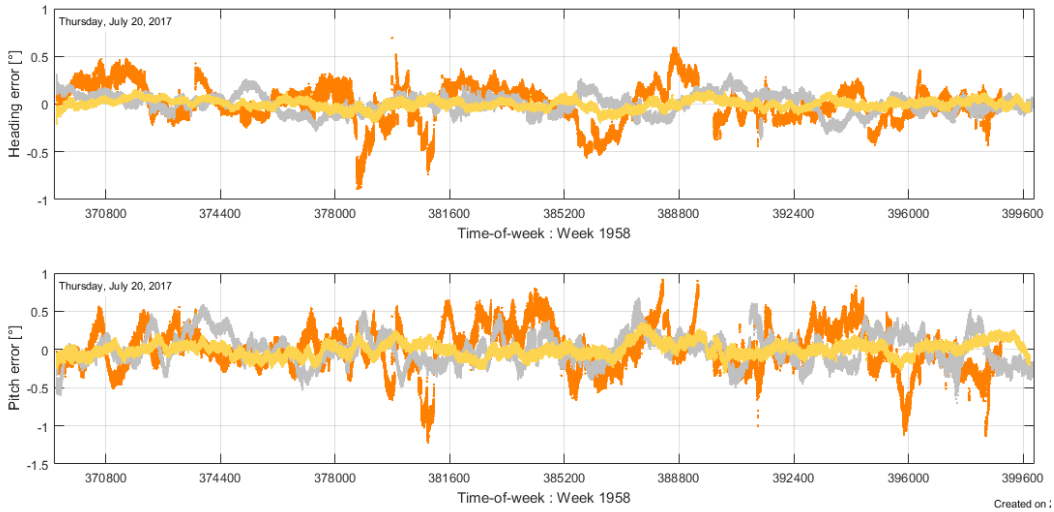

Figure 2: GNSS heading/pitch errors over time for PolaNt (yellow), Tallysman (orange), and Tallysman with ground plane (gray).

Table 2: GNSS heading/pitch RMS for PolaNt-MF, Tallysman and Tallysman with ground plane.

Antenna type	**Heading RMS (°)**	**Pitch RMS (°)**
PolaNt	0.05	0.09
Tallysman	0.20	0.28
Tallysman + ground plane	0.10	0.20

For the patch antenna without ground plane the heading RMS is four times higher than with a survey-grade antenna. For pitch it has an RMS about three times larger than the survey-grade antenna. If the ground plane is used, performance increases significantly. But the performance is still about two times worse for both heading and pitch.

GNSS antenna baseline comparison

The impact of the antenna baseline length on GNSS attitude is assessed by comparing the heading and pitch performance for different baseline lengths: 49 cm, 110 cm, and 207 cm. For each baseline 1 hour of data was recorded with a patch antenna (with ground plane).

Figure 3 shows the time plots for GNSS heading and pitch over time. The RMS values for the different baselines are given in Table 3. As expected, the RMS values decrease with increasing baseline lengths. This becomes more pronounced when looking at Figure 4, which shows the RMS with respect to the baseline length for heading and pitch.

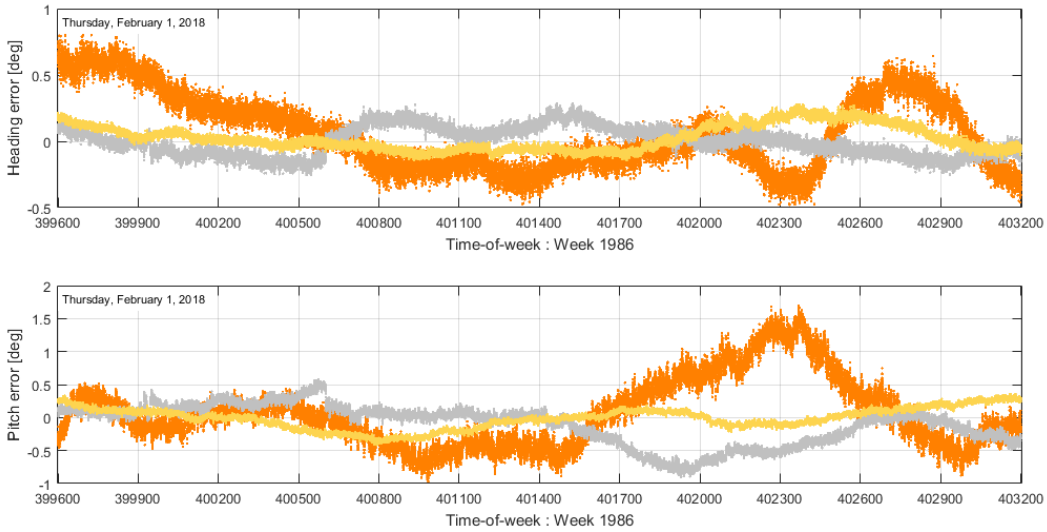

Figure 3: GNSS heading/pitch errors over time for baseline lengths of 49 cm (orange), 110 cm (gray), and 207 cm (yellow).

Table 3: GNSS heading/pitch RMS for baseline lengths of 49 cm, 110 cm and 207 cm.

Baseline length (cm)	Heading RMS (°)	Pitch RMS (°)
49	0.29	0.52
110	0.11	0.31
207	0.10	0.16

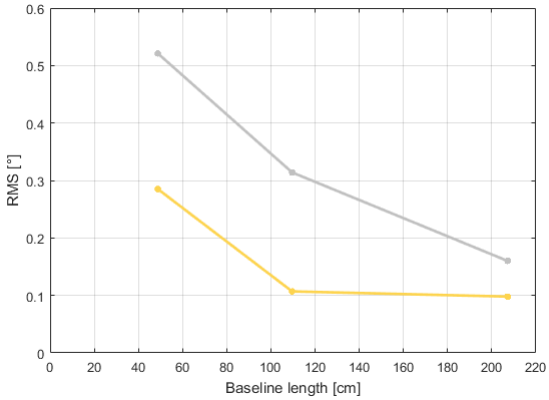

Figure 4: RMS of GNSS heading (yellow) and pitch (gray) with respect to baseline length.

SEPTENTRIO'S ASTERX-I

This section introduces Septentrio's new GNSS/INS product, the AsteRx-i, which combines robust and reliable cm-level RTK positioning with a light-weight industrial-grade IMU (< 15 g). The AsteRx-i consists of an AsteRx-m2a OEM GNSS receiver board connected to a MEMS IMU.

The AsteRx-m2a is a low-power dual-antenna GNSS receiver with multi-frequency multi-constellation tracking. With the INS capabilities it provides up to 100 Hz integrated position and attitude output with low latency (< 20 ms). The MEMS IMUs supported by the AsteRx-i are: the SBG Systems Ellipse Micro IMU (AsteRx-i *S*) and the VectorNav VN-100 IMU (AsteRx-i *V*). The two product variants are shown in Figure 5. The sensor specifications of the IMUs are given in Table 4. In the UAV test discussed in the next sections the *S* variant of the product was used.

Figure 5:AsteRx-i S (left) and AsteRx-i V (right).

Table 4: Overview of the AsteRx-i IMU specifications

Specifications	AsteRx-i S		AsteRx-i V	
	Accelerometers	**Gyros**	**Accelerometers**	**Gyros**
Input range	±16 g	±450 °/s	±16 g	±2000 °/s
Bias in-run instability	14 µg	7 °/h	40 µg	5 °/h
Noise density	57 µg/√Hz	0.15 °/√Hz	140 µg/√Hz	0.21 °/√Hz
Misalignment	< 0.05°	< 0.05°	< 0.05°	< 0.05°

UAV TEST SETUP

Overview of the UAV

The UAV used for the tests is a large X8 octocopter from the UAV manufacturer Stormbee. The UAV itself weighs 12 kg and can reach flight speeds of up to 15 m/s. It has two patch antennas fixed to the end of two booms, separating the antennas by approximately 2 m.

Figure 6: Stormbee S quadcopter.

By default, the UAV is equipped with a mount for a high-end Faro LiDAR. The UAV was modified to allow mounting an additional payload box next to the LiDAR. This rigid carbon-fiber box contains the MEMS IMUs under test. The total take-off weight (UAV, batteries, LiDAR and payload box) is 28 kg, resulting in about 7 min of flight time.

Payload description

The UAV payload box contains Septentrio's AsteRx-i S, two competitor systems and a high-end INS. Competitor 1 uses an IMU with specifications comparable to the IMU used by the AsteRx-i. For competitor 2 no IMU specifications are available, the complete GNSS/INS systems is about twice the price of an AsteRx-i. All systems support the use of GNSS heading to update their INS filter. The two antennas of the UAV are connected to splitters inside the payload box, so all receivers use the same antennas. An overview of the systems is given in Table 5.

Table 5: Overview of the tested systems

INS	IMU	GNSS receiver
Septentrio AsteRx-i	MEMS IMU	AsteRx-m2a
Competitor 1	MEMS IMU	AsteRx-m2a
Competitor 2	Integrated MEMS-based GNSS/INS	
Reference	High-end IMU	AsteRx-m2a

As described in the previous section the AsteRx-i consists of an AsteRx-m2a low-power dual-antenna GNSS receiver board with INS capabilities connected to a MEMS IMU. One of the competitor systems (Competitor 1) and the high-end reference INS need an external GNSS receiver to feed them with a GNSS solution (position, velocity, and heading). A separate Septentrio AsteRx-m2a receiver is used as external GNSS receiver for these systems. The other competitor system (Competitor 2) is a fully integrated GNSS/INS system with its own IMU and GNSS receiver.

Figure 7 shows a rendering of the payload box. There are three levels inside the box. Due to its weight, the high-end INS device is mounted on the highest level close to the UAV body. All GNSS/INS systems under testing, except Competitor 2, are mounted together on the level below to ensure that the systems under testing experience similar vibrations. Competitor 2 is built into the Stormbee UAV and is located on a vibration isolation mount on top of the UAV body. The bottom level houses the GNSS receivers and antenna splitters.

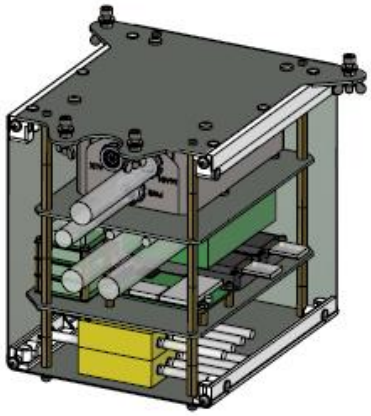

Figure 7: Rendering of the UAV payload box.

Environment and trajectory

The UAV flights were done at Aerodrome Liernu in Belgium as shown on Figure 8, a known testing ground for UAV manufacturers. The area has open-sky fields to allow straight and level flight, as well as sparse trees and a hangar for more challenging environments. For the flight campaign, we focused on a trajectory typical for LiDAR applications. For this use case, the UAV flies at relatively low speeds (< 5 m/s) and at low altitudes (< 20 m). The trajectory used during this test is a check pattern trajectory, typical for applications such as photogrammetry or laser scanning. It covers the survey area with overlapping point clouds. An example of such a trajectory can be seen in Figure 9.

Figure 8: View of the Liernu Aerodrome.

Figure 9: Trajectory of the UAV test flight, showing multiple passings of the barn (bottom) and concrete slab (right of the barn).

Most UAV applications requires GNSS RTK position accuracy. GNSS RTK is for instance necessary in case of laser scanning to accurately geo-reference the point cloud. Since this test campaign is aimed at benchmarking the performance of the different INS solutions in a real UAV test case, we will compare the INS solution performance using only GNSS RTK data. During the flights all receivers are provided with corrections from a local RTK network using a mobile broadband modem.

LIDAR REFERENCE CREATION

The UAV is equipped with a high-end Faro LiDAR. The recorded LiDAR measurements can be processed with each of the INS solutions, resulting in UAV LiDAR point clouds whose measurements are precisely time and space-located. The UAV flights are made over an area with good surface models. As a metric for the performance of the AsteRx-i and its competitors, we looked at how close the UAV point clouds are to a reference surface, as described in more detail in the next section.

To observe the INS performance using the LiDAR, we proceeded with the following steps:

- Step 1: Creation of a reference point cloud obtained by processing data from a static LiDAR mounted on a locally surveyed tripod (see Figure 10 on the left). The point cloud is geo-referenced using the GNSS position of the tripod averaged over 15 minutes. The LiDAR also scans several markers for which the absolute position is well known. These serve as additional anchor points for the point cloud.
- Step 2: Creation of a reference surface from the reference point cloud, by fitting a surface model in the point cloud by least-square regression (see Figure 10 on the right). This results in a fine-grained mesh of triangular surfaces.
- Step 3: Processing of the LiDAR measurements onboard the UAV with each one of the INS solutions (AsteRx-i and its competitors) to obtain one UAV point cloud per INS solution.
- Step 4: Computation of the error statistics of each point cloud relative to the predefined reference surface.

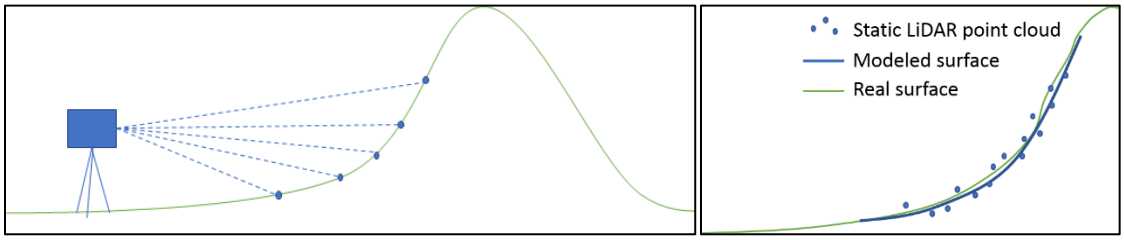

Figure 10: Step 1 (left) static point cloud creation, and step 2 (right) fitting a surface model.

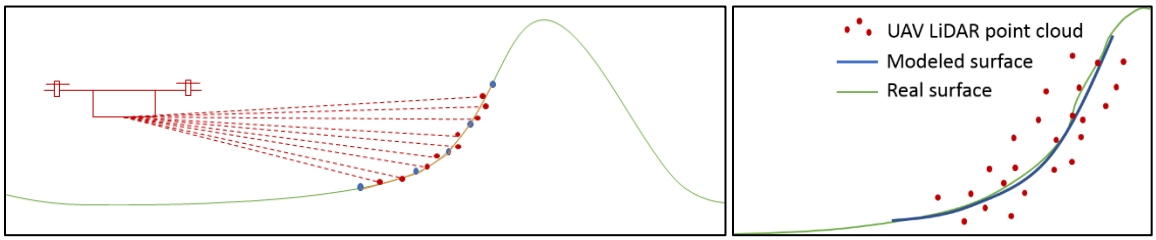

Figure 11: Step 3 (left) UAV point cloud creation, and step 4 (right) UAV point cloud error computation with respect to the modeled surface

It should be noted that the absolute georeferencing of the point cloud is not perfect and a bias between the rover point clouds and the reference point cloud is removed by rotating and translating the reference mesh to best fit the individual rover point clouds.

The statistics of the relative errors between the point cloud and the fitting surface are defined by the LiDAR and the INS accuracy. The typical error of the LiDAR laser is close to 0.5 cm. The averaged GNSS position associated to the static point cloud has an accuracy of 1 cm while the GNSS solutions on board the UAV will cause point cloud position errors up to:

- 4 cm typical error due to the horizontal RTK position RMS with patch antennas in kinematic conditions.
- 6 cm typical error when considering typical 0.15° heading error with a 20 m laser range.

The modeled surface accuracy depends on the LiDAR accuracy (0.5 cm) and on the averaged GNSS static position accuracy (1 cm). Considering that the LiDAR ranging errors are only white noise and considering that we scanned simple surfaces (horizontal and vertical plans) the noise on the LiDAR measurements should not influence the modeling of the modeled surface by Least-Square regression. We will thus neglect the influence of the LiDAR accuracy on the modeled surfaces. Only the averaged GNSS position error will have influence on the absolute accuracy of the modeled surface.

The accuracy error due to the LiDAR (1 cm) on board the UAV is much smaller than the sum of the errors (10 cm) due to the INS solution, so the errors of the point cloud with respect to the modeled surface are mainly influenced by the accuracy of the INS solution. We can consider that the point cloud provides a good observation of the INS solution accuracy (position and attitude).

UAV TEST RESULTS

During three consecutive flights, point clouds were created with the LiDAR for three different features in the landscape: the door and roof of a nearby barn, and a concrete slab. From the trajectory shown in Figure 9 it is clear that multiple passes per flight are made at each feature, so in total there are many overlapping point clouds containing the feature. The three reference surfaces can be seen in Figure 12. The reference surface mesh is shown in grey, and the total point cloud gathered through each pass are shown in color.

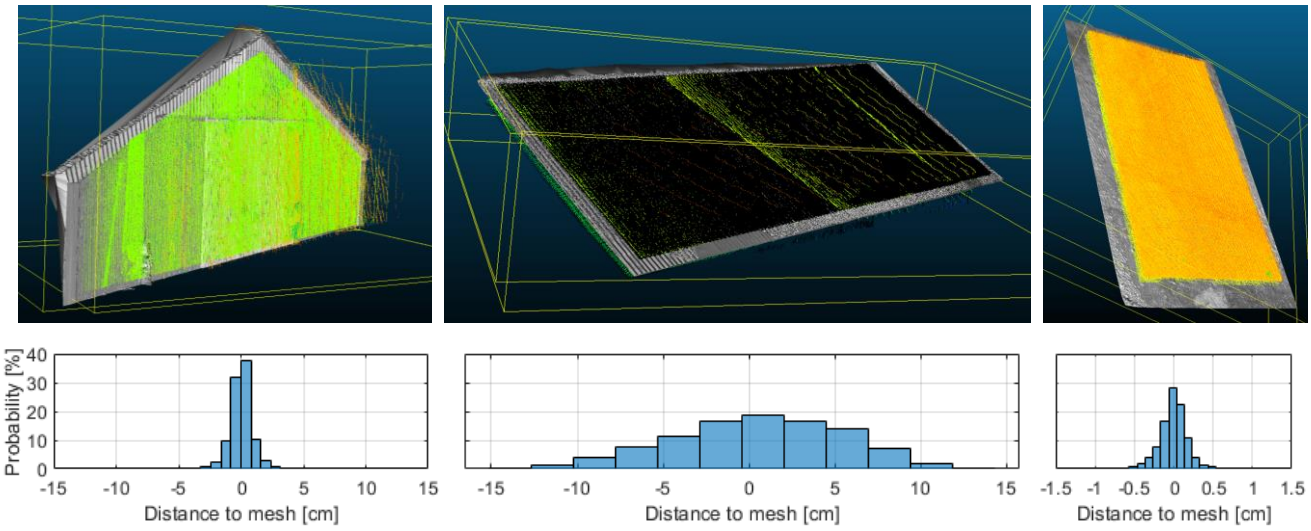

Figure 12: The top panels show three reference surfaces used in the performance assessment. The bottom panels show the distribution of the reference point cloud distances to the reference mesh, indicative of the reference quality. From left to right, we see the barn door, barn roof and concrete slab.

A Euclidean distance can be computed between each point and the triangulated surface mesh, and a sign can be associated to this distance depending on whether the point is more east-north-up of the surface (positive) or west-south-down (negative). Next we compute the 68% and 95% percentiles of the (unsigned) distances. The results of this analysis are shown in Table 6 for the 68% error percentile and Table 7 for the 95% error percentile.

Table 6: Error percentile at 68% of the point clouds for systems under test in cm.

Feature	AsteRx-i	Competitor 1	Competitor 2
Barn door	14.0	16.8	4.0
Barn roof	20.9	21.5	9.8
Concrete slab	18.1	19.2	5.5

The 68% percentile of the distances between the points and the reference surface computed from the static ground scans is an indicator of the typical error introduced by the position and attitude accuracy of the GNSS/INS system with which the point cloud is geo-referenced. Hence, this metric provides an alternative assessment of the accuracy of the GNSS/INS system. In general, the AsteRx-i is more accurate than competitor 1 which uses an IMU with similar specification. The integrated GNSS/INS system of competitor 2 is performing consistently better than both other systems with this metric. As stated in the setup section, competitor 2 is a more expensive system and is better placed on the rigid body of the UAV on a vibration isolation mount.

Table 7: Error percentile at 95% of the point clouds for systems under test in cm.

Feature	AsteRx-i	Competitor 1	Competitor 2
Barn door	121	125	46.4
Barn roof	55.8	61.1	23.9
Concrete slab	108	107	101

The 95% percentile is a measure of the tail of the distance distribution of the point cloud and indicates the consistency of the georeferencing over multiple passes and multiple flights. It is therefore a measure of the repeatability of the LiDAR measurement geo-referenced with the GNSS/INS system. Again, we can see that the AsteRx-i scores as good as or better than competitor 1 and that competitor 2 is showing better performance. For this metric however, the difference between competitor 2 and the other systems for the concrete slab point cloud is not as pronounced.

CONCLUSIONS

This paper described an assessment of a new MEMS-based RTK/INS system, specifically for UAV applications. The recent rise in the use of UAVs for a variety of applications such as LiDAR, photogrammetry and survey applications has created a need for light-weight GNSS/INS systems that are robust and reliable but meet the accuracy requirements of such applications. The small formfactor of UAVs compared to traditional machine control applications means that the antennas used for GNSS position and attitude computation are small and positioned relatively close together. Therefore, this paper discussed the impact of the antenna type and of the antenna baseline on the accuracy of the GNSS solution which drives the INS. A popular patch antenna model shows a twice larger position error RMS value compared to a survey grade antenna, while adding a metal ground plane reduces that to a fifty percent larger RMS value. The position error of the GNSS engine directly impacts the position accuracy of the INS. GNSS attitude estimation with two antennas can greatly reduce the convergence time of the INS and can improve attitude accuracy during low dynamics (e.g. hovering, straight and level flight). Reducing the antenna baseline from 2 m to 50 cm leads to a threefold increase of heading error RMS value and more than threefold increase for pitch.

This paper introduced Septentrio's new RTK/INS system based on pairing an industrial grade MEMS IMU with a dual antenna RTK GNSS receiver, called the AsteRx-i. It also described an approach to use a LiDAR mounted under a commercial UAV platform to compare the accuracy of this GNSS/INS with competing products. This assessment is carried out by comparing LiDAR point clouds recorded during flight and geo-referenced with each of the GNSS/INS systems under test with reference surfaces recording with the same LiDAR during static scans on the ground. This assessment shows how close the recorded point clouds are to the reference if the LiDAR data is tagged with Septentrio's AsteRx-i compared to a competing product which is based on a MEMS IMU with similar specifications as the IMU used for AsteRx-i.

ACKNOWLEDGEMENTS

The authors are grateful to the team of Stormbee for modifying the UAV to fit the payload box, and for their assistance during the test campaigns. The authors also would like to thank Wim De Wilde and Dirk De Vriendt at Septentrio for their help in preparing the UAV payload, and Jens Goemaere at Septentrio for his help in preparing the GNSS attitude baseline results.